The International Journal of Advanced Manufacturing Technology (2018) 96:881–894
https://doi.org/10.1007/s00170-017-1480-x

ORIGINAL ARTICLE

Colour quality of facial prostheses in additive manufacturing

Ali Sohaib[1,2] · Kinjiro Amano[1,3] · Kaida Xiao[4,5] · Julian M. Yates[1] · Charles Whitford[6] · Sophie Wuerger[4]

Received: 16 August 2017 / Accepted: 12 December 2017 / Published online: 1 February 2018

Abstract

Recent progress in additive manufacturing technology has improved the realistic colour reproduction of 3D facial prostheses with computational optimisation of skin colour profiles. The colour appearance of the prosthetic surface depends on both the spectral characteristics of the surfaces and the scene illumination. Considering everyday environments, the colours of prosthetic surfaces should appear constant under various illuminations, although such evaluations on facial prostheses have had limited success to date. In this study, colour quality was assessed throughout the additive manufacturing process, namely, from the colour profile optimisation to the colour reproduction on the 3D facial prostheses. Colour profiles optimised for typical skin colour samples were applied to manufacture facial prostheses with two skin types, Caucasian and Chinese. The colour quality was assessed by the colour difference metric CIEDE2000 and spectral similarity against corresponding real skin data. The constant colour appearance of the prosthetic surfaces under different illuminations was estimated by introducing a reproduction colour-constancy index. The CIEDE2000 between the prosthetic and real skins was approximately 7.2 on average over all skin types and facial areas, which is slightly larger than the acceptable perceptual error. The level was relatively constant under different illuminations selected from the CIE standard daylight and fluorescent lights. The reproduction colour-constancy index ranged from 0.34 to 0.89, which is remarkably similar to the level observed in traditional colour constancy data in vision sciences. Spectral errors were close to those obtained by computational spectral reconstruction from digital RGB colours. These results suggest that the proposed colour management for facial prostheses may satisfy the requirement of colour quality in everyday environments with various illuminations. The causes and further improvement of the remaining errors in the manufacturing process are also discussed.

Keywords Human facial prostheses · 3D colour printing · Skin colour, colour management · Perceptual error · JND · DeltaE

Nomenclature

CCT	Correlated colour temperature
CIE	International commission on illumination
CIELAB	CIE L*a*b* uniform colour space
CIEDE2000	CIE DE2000 colour difference formula
CRI	Colour rendering index
ΔE^*_{ab}	Colour difference unit calculated by CIELAB
ΔE^*_{00}	Colour difference unit calculated by CIEDE2000 colour difference formula

✉ Kaida Xiao
k.xiao1@leeds.ac.uk

[1] School of Medical Sciences, Division of Dentistry, University of Manchester, Manchester, UK

[2] School of Science & Technology, Nottingham Trent University, Nottingham, UK

[3] School of Electrical and Electronic Engineering, University of Manchester, Manchester, UK

[4] Department of Psychological Sciences, University of Liverpool, Liverpool, UK

[5] The School of Design, University of Leeds, Woodhouse Lane, Leeds, UK

[6] School of Engineering, University of Liverpool, Liverpool, UK

1 Introduction

The colour of skin can provide essential information about an individual's health and emotional state [1–3]. Facial cues and facial expression including colour are important factors in social communication [4, 5]. Furthermore, the human colour vision system appears to be sensitive to subtle changes in skin colour and thus can gain important information from any variations in colour [6, 7]. For these reasons, it is important to achieve precise colour reproduction on skin prostheses as a natural and "life-like" look is paramount for both patient and society as a whole.

The demands in manufacturing maxillofacial prostheses have been increasing [8] along with the technological developments in additive manufacturing [9, 10]. Within applications in clinical and medical practices, for example, skin defects may be replaced with additively manufactured prostheses to provide functional rehabilitation and aesthetic improvements. Good prosthesis quality may also bring associated improvements in social, emotional and psychological status, and overall quality of life [8] (see also [11–13]). Such requirements in prosthesis manufacturing are often compromised aesthetically and functionally because of the current limits in colour reproduction methods and materials. Colour management, which is the ability to reproduce colours precisely on facial prostheses, along with its control, is one of the critical factors in any of the manufacturing processes. In additive manufacturing, the limits on achieving high precision in colour reproduction depend on the physical properties of the materials, such as the spectral characteristics [14, 15], their compatibility with colour pigments in the printing system and their availability [16, 17].

Several innovative methods have recently been reported to achieve accurate 3D colour reproduction [9, 18, 19]. These methods optimise colour profiles by applying a computational learning algorithm to reference colour samples and the target colours. Xiao et al. (2016) used the International Commission on Illumination (CIE) tristimulus values to represent colours on a specially designed collection of skin colour samples for computational optimisation [10]. The collection of colour samples covers the variations in target skin tones of a specific skin type or ethnicity [20] (see also [21]). Thus, the selection of samples colours may determine the quality of colour reproduction.

Despite the technical and engineering progress made in additive manufacturing, there is no systematic method to assess the colour fidelity and quality of facial prostheses in the additive manufacturing process. Furthermore, the measurement of colours on real and 3D facial prosthetic surfaces is often difficult due to variations in their physical properties, such as geometry and texture [22–25]. Colours are represented by triplets of colour standard values or chromaticity coordinates [26]. However, colour is also determined by the spectral characteristics of surfaces and illumination. Thus, assessments of colour quality must account for both colorimetric and spectral evaluations. A common approach in colorimetric evaluation is to measure perceptual error, namely, a colour difference metric, between the prostheses and the original skin colour [26, 27]. In contrast, spectral evaluation can be performed by comparing spectra between the reference and target surfaces. Among several proposed metrics, the root mean square error (RMSE) and spectral similarity value (SSV) have been commonly used [28, 29]. Furthermore, it is necessary to assess the colours under different illuminations. Consistent colour appearance of a surface under different illuminations is an important factor in manufacturing facial skin. The notion of "colour constancy" in vision sciences represents a phenomenon in which the colour appearance of surfaces is invariant despite changes in illumination: for example, the colour of a surface under sunlight is colorimetrically different from the colour of the same surface under a room light, but perception of the surface colour is approximately constant. Achievement of colour constancy on prosthetic surfaces should be a practical requirement for facial prostheses produced by additive manufacturing.

The colours of manufactured surfaces must be compared with those of real skin, in relation to normally occurring variations in skin colour. The colour of skin varies between and within ethnic groups [21], age and gender [30, 31] (see also [32]). Perceptual colour differences are typically measured with colour difference formula (ΔE) in the CIE 1976 $L^*a^*b^*$ colour space (ΔE^*_{ab}) or CIEDE2000 [27, 33]. Xiao et al. (2017) reported that the perceptual colour difference ranged from 4.3 to 6.2 in ΔE^*_{ab} units across different skin types and body areas [21] (see also [34]).

With manufactured skin prostheses, Paravina et al. [8] reported that the perceptibility and acceptability thresholds for colour differences in skin coloured maxillofacial elastomers were not more than 4.4 and 3.1 with ΔE^*_{ab} and CIEDE2000, respectively. However, their estimates were not extended to include the effect of illumination. Apart from manufactured skin, colour matching in dental teeth shade guides has also been extensively studied [30, 35]. Similar to skin colours, the colours of teeth vary with individuals (the structure and components of teeth, such as the thickness and translucency of dentin and enamel, affect the absorbance and reflection of light), patient age and colour of the surrounding skin or lips. The effect of illumination has been reported to affect appearance of teeth [25]. To clinicians, colour differences ranging from 2.6 to 5.5 ΔE^*_{ab} are visible [36]. Additionally, the ranges of colour difference ΔE^*_{ab} under different illuminants were similar to those of the dental shade guide; ΔE^*_{ab} was approximately 3.0, with the CIE standard illuminants A, D65 and F2 [25].

These results may serve as a baseline to assess the colour quality of prosthetic skin surfaces in additive manufacturing. However, the assessments have not been conducted throughout the entire additive manufacturing process. The present study aims to assess colour quality from the digital image acquisition of human faces to the production of the corresponding facial prostheses in additive manufacturing with an elaborate colour management method. Colour quality has been assessed colorimetrically and spectrally. The spectral errors in the manufacturing process will be evaluated by the RMSE and spectral similarity value (SSV).

This article consists of three parts. First, a colour management pipeline in the additive manufacturing of 3D facial skin prostheses with an optimised colour profile is introduced.

Second, the colour qualities of facial prostheses with two different skin types, Caucasian and Chinese, are assessed by colorimetric and spectral errors relative to the corresponding real skin surfaces. Third, colour appearance under different illuminations was estimated by simulating various illuminations, and their constant colour appearance was estimated by introducing a reproduction colour-constancy index.

The PANTONE Skin Tone Guide was used as a colour template to generate the skin colour profile in the manufacturing process [20]. Accuracy and consistency of colour management was verified with a comparison between the reproduction of the PANTONE Skin Tone Guide and the original. The colorimetric assessment was performed with the CIE colour difference metric CIEDE2000 [27, 37], and the spectral difference was assessed by the RMSE and SSV between the manufactured prosthesis and original real skin. The effects of illuminations were computed from the illumination by daylight and fluorescent lamps defined by the CIE (e.g. D65, A, F2 and F11) [38]. Colour constancy of the manufactured skin was assessed by a colour reproduction index, equivalent to the conventional colour-constancy index established in vision sciences [39].

The results highlighted notable variations in colours and spectra between the three human subjects, local areas and skin types. However, the colorimetric and spectral evaluations indicate that colour perceptual errors between the facial prostheses manufactured through the proposed colour management pipeline and corresponding real skin surfaces are close to the acceptable level of error [8, 40]. The reproduction colour constancy of the additively manufactured skin under selected illuminants was similar to those obtained by traditional colour constancy experiments with human observers [e.g. 43,41].

The remainder of this article is organised as follows. Section 2 provides general information about experimental materials and methods. Section 3 provides a brief review of the manufacturing procedure of facial prostheses, including colour management established with the optimisation of colour templates. Section 4 assesses the reproduction of colour templates by additive manufacturing. Sections 5 reports the colorimetric assessments of the 3D and 2D facial prostheses manufactured for Caucasian and Chinese skin types. The effect of various illuminations on colour appearance was estimated by introducing the reproduction colour-constancy index. Section 6 analyses the spectral characteristics of the prostheses. Finally, section 7 discusses the cause of errors in the manufacturing process and considers ways to improve the quality of colour in 3D additive manufacturing.

For convenience, this study refers to the spectral reflectances measured on the physical PANTONE Skin Tone Guide [20] as "ground-truth chart" and those of the real skin data as "ground-truth skin" in the following sections.

2 Materials and methods

2.1 Apparatus

Spectral reflectances of human skin and additively manufactured facial prostheses were measured with a portable spectrophotometer (Konica Minolta CM-700d, Tokyo, Japan) for both of the skin charts, human facial skin and the manufactured facial prostheses of the corresponding human subjects. Prior to taking measurements, the spectrophotometer was calibrated in accordance with the manufacturer's recommendations, and white and dark calibrations were performed. The white calibration involved measuring the light intensity of a spectralon white sample, whereas the dark calibration involved recording the stray light without any sample in front of the measurement port of the CM700d. The spectrophotometer measured the spectrum for wavelengths ranging from 400 to 700 nm in 10-nm increments. The aperture size was set to 3 mm for all measurements. (The details of the configuration have been described previously [41].) The spectral reflectance measurements have a standard deviation of less than 0.1%, and the colorimetric value ΔE^*_{ab} has a standard deviation of 0.04.

For the manufactured prostheses, 3D geometry and 2D colour information were acquired by dedicated digital imaging systems [10, 42], namely, the 3dMD facial imaging system (3dMD, Atlanta, GA, USA) and Spectrum Z510 3D printer (Z Corp, Burlington, MA, USA).

2.2 Simulated illuminants

Skin colours under various illuminations as well as CIE daylight D65, a colorimetric standard, were calculated. The simulated illuminants ranged from daylights to fluorescent lamps: the CIE daylights D65 and D50, illuminant A and three types of CIE fluorescent illuminants (F2, F7, F11). Illuminant D65 corresponds to average noon daylight with a correlated colour temperature (CCT) of approximately 6500 K and is defined as the standard illuminant for colorimetric calculations [38]. Illuminant D50 corresponds to slightly warmer white light, with a CCT of approximately 5000 K, and is often used as a reference in the graphics industry. Illuminant A represents a domestic incandescent or tungsten lamp with a CCT of approximately 2860 K. The fluorescent illuminant F2 is a common fluorescent lamp used for typical office illumination and is "cool white fluorescent", with a CCT of approximately 4200 K. Illuminant F7 is a broadband fluorescent lamp that is an approximation of illuminant D65 with a higher colour rendering index (CRI = 90). Illuminant F11 has three narrow peaks over the visible spectrum [26], with a CCT of approximately 4000 K, and is mainly used as warehouse lighting.

2.3 Human subjects

Measurements of the facial skin reflectances were collected from three human subjects, one with Caucasian skin (female, age 18) and two with Chinese skin types (two males, aged 21 and 40). All three subjects were based at the University of Liverpool and volunteered for facial measurements.

The facial prostheses of the three subjects were manufactured from the 3D and 2D digital images of their faces obtained by the dedicated imaging systems. The digital imaging procedures are summarised in Sect. 3 [42].

All experiments were conducted following approval by the University of Liverpool Research Ethics Committee, which operates in accordance with the Declaration of Helsinki. Signed consent was obtained from each subject who took part in the measurements.

2.4 Measurement protocol

The spectral reflectances of the forehead and cheek regions of each subject's face and their respective prostheses were measured with the spectrophotometer. The procedure for measuring real human skin followed the protocol established earlier [41, 43]. None of the subjects wore any cosmetics at the time of measurement. On the facial prostheses, the measurements were taken on three regions of the face, on the forehead and cheek, with the spectrophotometer. Whilst the forehead measurement was taken near its central area, for the cheek, two or three different areas were measured and averaged. For both real skin and the prostheses, any area with a mole or unusual pigmentation or markings on the skin surface was avoided. Spectral measurements on the Skin Tone Guide and Skin Colour Chart were also performed on the 110 colour samples.

3 2D and 3D printing protocol

3.1 Procedure for generating skin prostheses

The protocol for skin reproduction with facial prostheses, including the acquisition of 3D geometric data by digital imaging, has been summarised previously [10]. However, briefly and for clarification, the protocol consisted of the following steps. The first step was to perform 3D scanning of the subject's face using a 3D photogrammetry system in order to capture the 3D topography [10]. The 2D digital images from the cameras were then transferred onto the 3D model utilising texture mapping involving the 3dMD software. Each polygon in the 3D mesh obtained its colour from the 2D image. Therefore, the transformation is only applied to the 2D colour image that is common to both the 2D and 3D prints.

The resulting mesh data were then manually edited to remove noisy polygons and unwanted regions around the face. This was because specular highlight on the surface, occlusion of light or accidental shadows would have generated errors in the scanning process and therefore the subsequent polygons. The data was edited using a combination of available software suites (Materialise Magics 19.01, Materialise, Leuven, Belgium; Blender 2.78, https://www.blender.org). Additionally, finer texture adjustments on the surfaces of the prosthesis were added to make the surfaces more realistic for the next step in the process. Finally, adjustments were made according to the technical requirements for the prosthesis, such as the thickness required for the shape to be held rigidly and the supports needed to practically apply the prostheses to the patients. In the manufacturing process, silicon medical-grade powder ZP 15E (Z Corp, Burlington, MA, USA) was used in the 3D printer (Spectrum Z510, Z Corp, Burlington, MA, USA) [16].

3.2 Colour management

Conventional colour image reproduction techniques based on the CIE colorimetry protocol have been used to transform colour images from one medium to another under various viewing conditions [26]. However, the application to 3D printing technology requires careful considerations due to the changes in colour and illumination geometries.

To achieve better colour management in 3D skin reproduction (e.g. high colorimetric accuracy), a complex and bespoke colour profile has been developed for skin colours, namely, the skin colour chart with computational optimisation [10].

Colour management was undertaken throughout the entire additive manufacturing process, that is, from the 3D image acquisition by the 3dMD camera to the 3D printing by the ZCorp 3D printer. Traditional polynomial regression using the least-squares method [33] and the 3D thin plate spline method (3D TPS) [44] were tested. The 3D TPS was originally developed for geometric transformation, but it was applied to the colorimetric data (e.g. CIE tristimulus values XYZ and RGB digital image data) in this study.

The transformation between the RGB values and CIE tristimulus values XYZ at the digital image acquisition stage by the 3dMD camera and the 3D printing by the ZCorp printer were obtained with the ColorChecker Digital SG (X-Rite Pantone, Grand Rapids, MI, USA), as shown in Fig. 1a. The CIE tristimulus values XYZ of the ColorChecker Digital SG charts were obtained by a spectrophotometer and were transformed using 3D TPS and polynomial regression.

In order to optimise the process, the camera used an RGB to CIE XYZ transformation, which was obtained by scanning the ColorChecker Digital SG chart using the 3DMD system and then obtaining the Tristimulus values of the chart using CM700d. Furthermore, the transformation for the printer (CIE XYZ to RGB) was obtained by printing the same chart and obtaining the resulting CIE XYZ values of each colour patch

using CM700d. For the printing, a colour image from a 3D scan first undergoes camera transformation (RGB to CIE XYZ), and then the final printer RGB values are obtained using the second transformation for the printer, i.e. CIE XYZ to RGB.

Polynomial regressions based on first-, second- and third-order polynomials were then tested. For n training colours in the ColorChecker Digital SG chart, the terms used for polynomial regression are defined by the Matrix E (nx3):

	Polynomial terms
1st order	[E]
2nd order	[E_1 E_2 E_3 E_1^2 E_2^2 E_3^2 E_1E_2 E_1E_3 E_2E_3 1]
3rd order	[E_1 E_2 E_3 E_1^2 E_2^2 E_3^2 E_1E_2 E_1E_3 E_2E_3 E_1^3 $E_2{}^3E_3{}^3$ $E_1^2E_2$ $E_1^2E_3$ $E_2^2E_1$ … …. $E_2^2E_3$ $E_3^2E_1$ $E_3^2E_2$ 1]

The 3dMD uses the camera's built-in flash light, which has a correlated colour temperature of approximately 5500 K, and the colorimetric measurement by the spectrophotometer was based on D65 illuminant (correlated colour temperature of 6500 K). The difference was compensated for in the camera colour characterisation model.

The 3D TPS method uses an affine transformation A (linear distortion) along with a weighting factor W that controls the nonlinear distortion for the transformation of XYZ and RGB:

$$\begin{bmatrix} K & P \\ P^T & O(4,4) \end{bmatrix} \begin{bmatrix} W \\ A \end{bmatrix} = \begin{bmatrix} V \\ O(4,3) \end{bmatrix},$$

where V is the reference matrix for n data points, P is the matrix to be warped and O is a matrix of zeros. The x,y,z variables in matrix V and P can take values of RGB and XYZ interchangeably depending on whether the transformation is for camera or printer.

$$V = \begin{bmatrix} \hat{x_1} & \hat{y_1} & \hat{z_1} \\ \dots & \dots & \dots \\ \hat{x_n} & \hat{y_n} & \hat{z_n} \end{bmatrix}$$

$$P = \begin{bmatrix} 1 & x_1 & y_1 & z_1 \\ \dots & \dots & \dots & \dots \\ 1 & x_n & y_n & z_n \end{bmatrix}$$

K defines the nonlinearity between RGB and XYZ.

$$K = \begin{bmatrix} 0 & U_{r_{12}} & \dots\dots & U_{r_{1(n-1)}} & U_{r_{1n}} \\ U_{r_{21}} & 0 & \dots\dots & U_{r_{2(n-1)}} & U_{r_{2n}} \\ \dots & \dots & \dots\dots & \dots & \dots \\ U_{r_{(n-1)1}} & U_{r_{(n-1)2}} & \dots\dots & 0 & U_{r_{(n-1)n}} \\ U_{r_{n1}} & U_{r_{n2}} & \dots\dots & U_{r_{n(n-1)}} & 0 \end{bmatrix},$$

where

$$r_{12} = \sqrt{(x_2 - x_1)^2 + (y_2 - y_1)^2 + (z_2 - z_1)^2},$$
$$U_{(r_{12})} = 2(r_{12})^2 \log(r_{12}).$$

Colour profiles of the devices were developed using each of these methods, and the colour difference between original chart and the printed one was calculated using the CIEDE2000 [33, 37], ΔE^*_{00} (Table 1).

Based on the colour difference ΔE^*_{00}, the third-order polynomial regression and 3D TPS were further evaluated in terms of their suitability for printing skin colours with The PANTONE Skin Tone Guide [20].

A colour chart made from the PANTONE Skin Tone Guide was used to validate the optimisation (Fig. 1b). The skin colour chart based on the PANTONE Skin Tone Guide [20] covers the majority of skin tones, such as whitish, yellowish and brownish, including Caucasian and Chinese skin types, with a total of 110 skin tones. Each colour chip was printed with a lacquer coating on paper. The 110 skin tones were aligned in a 10 × 11 matrix and had dimensions of approximately 20 mm × 10 mm. A manufacturing pipeline on a 2D plate [16] was then used to generate the skin colour chart.

The skin colour chart was then scanned by the 3dMD camera and printed by the 3D printer with both the third-order polynomial regression and 3D TPS.

Colorimetric measurements on the printed colour chart were then performed with the spectrophotometer, and colour differences from the corresponding colours in the original skin chart were calculated in the CIEDE2000. The ΔE^*_{00} values are listed in Table 2.

The mean colour difference for the 3D TPS method was 3.56, which was smaller than the figure gained using third-order polynomial regression. Therefore, the 3D TPS method was selected for printing the facial prostheses.

3.3 Procedure for manufacturing facial skin

The 2D and 3D manufacturing used the same colour management established by the Skin Tone Guide, as described earlier in the Sect. 3.1 (see also [10]).

The subjects were imaged by the 3dMD scanner, which provides dense 3D special resolution mesh surface topography with 2D colour information. The 2D digital image was 4062 × 4574 pixels in size after integrating the images from the three cameras. The software for the 3dMD system then performs texture mapping to overlay the 2D colour

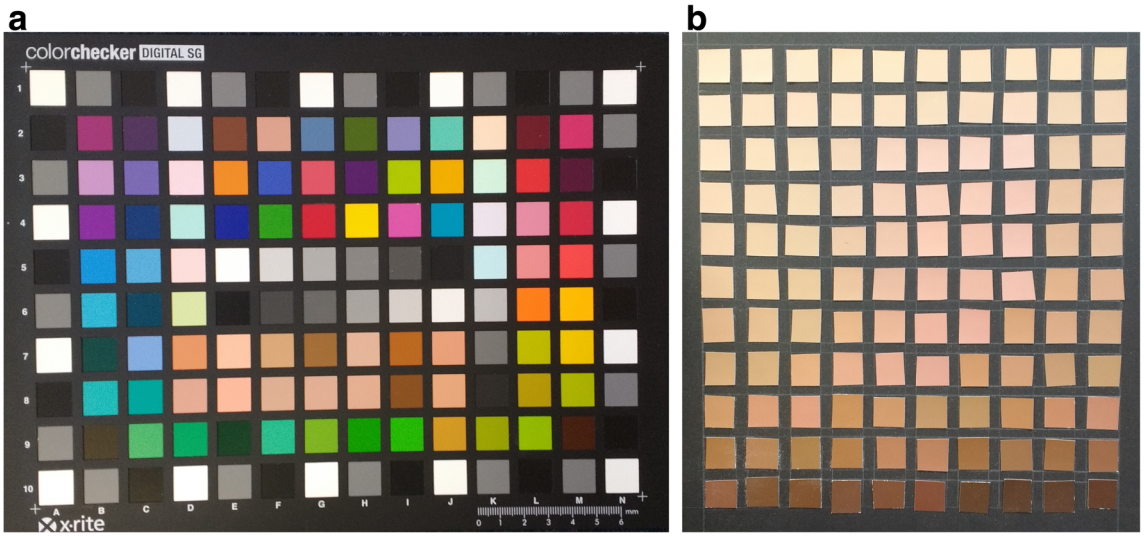

Fig. 1 **a** ColorChecker Digital SG used to calibrate the 3dMD camera and ZCorp 3D printer. **b** Colour chart made from the PANTONE Skin Tone Guide [20], used to evaluate overall colour management

information of the object (face) acquired from three different angles onto the 3D mesh model.

Image "noise" was then edited or removed with the 3D-model editing software Materialise Magics (19.01) to create the final 3D model. The final 3D model includes an additional thickness on the surfaces to make it more brittle. The thickness varied from 1.5 to 3 mm.

The colour information of the skin surfaces was transformed using the 3D TPS method. A single transformation was applied to both the 2D flat printed face and 3D face model because both used the same 2D image. Once the transformation was applied to the 2D image, the model was ready for printing. Printing was undertaken using the ZCorp spectrum 510 printer with a starch- or cellulose-based powder (ZP15e). The thickness of each printed layer was set to 125 μm. The entire printing process typically takes 60 min although the exact duration varies with the size of the object (prostheses) and the number of layers printed.

At the end of the printing process, the printed parts required infiltration with medical-grade silicone to add overall flexibility and strength (S-25 Techsil 25 Addition (Platinum) Silicone Rubber, Technovent Ltd, Bridgend, UK). Following infiltration, the models were then allowed to fully dry for 12–16 h. In order to keep similar colour profiles for training and for printing skin models, the infiltration process was also carried out during the colour management process.

Table 1 Training error for each of the transformations

CIE ΔE^*_{00}	Mean	Max.	Min.	Std. dev.
1st order	5.3447	27.3794	0.8707	4.3172
2nd order	4.1966	19.9726	0.5476	3.2466
3rd order	3.6720	18.7609	0.4689	2.9681
3D TPS	1.5615	9.8135	0.0614	1.8586

4 Analysis of the skin chart

4.1 Colorimetric analysis

To assist in the evaluation of the additive colour manufacturing in this report, the data from our earlier results were compared with those of the three subjects. Xiao et al. [21] previously reported the distributions of chromaticities in colour space based on a large database of measurements of 960 human subjects including Caucasian and Chinese samples. This study reports the data of 249 Caucasian and 277 Chinese samples with additional measurements. The distributions of the CIE 1976 a^*b^* chromaticities of human subjects' skin under the CIE standard illuminant D65 are shown as convex contours in Fig. 2a, and those of Chroma and L^* are shown in Fig. 2b. The distribution of chromaticities is referred to as the *colour gamut* in the remainder of this article.

The colour gamut of the 110 samples of the PANTONE Skin Tone Guide and their reproduction, the Skin Colour Chart, are shown in Fig. 2a, b for comparison. The colour gamut of the PANTONE Skin Tone Guide overlapped with that of the real skin colours of both Caucasian and Chinese

Table 2 Colour differences between the original and 3D printed Pantone chart using the two methods

CIE ΔE^*_{00}	Mean	Max.	Min.	Std. dev.
3D TPS	3.5536	6.9344	0.9299	1.1835
3rd order	3.9584	9.4959	0.7588	1.7419

skin. However, the colour gamut of the reproduction tones in the skin colour chart was considerably larger than the original PANTONE Guide, and expanded towards higher values in a^* and b^*, namely, redness and yellowness, in Fig. 2a, and thus higher chroma in Fig. 2b. Therefore, the manufactured skin tones shifted towards more saturated colours by the manufacturing pipeline (Sect. 3).

Colorimetric and spectral evaluations between the manufactured skin colour chart and the original Skin Tone Guide (ground truth) can represent the quality of the colour reproduction through the established pipeline.

The colorimetric difference between the original (ground truth) and manufactured skins was assessed with a colour difference metric, CIEDE2000 [27, 37], corresponding to perceptual error through standard human colour vision [27, 33, 37]. Under the CIE standard illuminant D65, the value of CIEDE2000, averaged over the 110 colour samples, was 3.6 (SD 1.18). This value was fractionally larger than the acceptable discernible range [8, 17]. (Note: in the simulation, the values of ΔE_{ab}^* are similar when $\Delta E_{ab}^* < 10$.) Details of the possible causes of these colour errors are provided in the discussion.

4.2 Spectral analysis

The spectral profiles of the original Skin Tone Guide and the skin colour chart are shown in Fig. 3a, b. The difference between their spectra can be assessed with the RMSE and SSV [29, 42], as defined in the following sections.

4.2.1 Spectral characteristics

The evaluation of the spectral differences between two spectra, the original and test spectra, can be performed with the RMSE and SSV [29, 42]. The definitions are given below. Denote the original spectrum as r_r and the test spectrum as r_t.

$$RMSE = \sqrt{\frac{1}{n}\sum_{i=1}^{n}\left(r_{r,i}-r_{t,i}\right)^2}, \tag{1}$$

$$\mathrm{SSV} = \sqrt{RMSE^2 + S^2}, \tag{2}$$

where n is the number of components of the reflectance. The square of S is defined by

$$S^2 = 1-\left[\frac{\left\{\frac{1}{n}\sum_{i=1}^{n}\left(r_{r,i}-\mu_r\right)\left(r_{t,i}-\mu_t\right)\right\}}{\sigma(r)\,\sigma(t)}\right]^2. \tag{3}$$

where μ_r and μ_t are the means of the reconstructed and original reflectances, respectively, and $\sigma(r)$ and $\sigma(t)$ are the standard deviations of the reconstructed and original reflectances, respectively.

4.2.2 Spectra of the skin chart

The spectral characteristics of the surface reflectances in the PANTONE Skin Guide and those additively manufactured with the colour profile are compared in Fig. 3. The spectra of the manufactured surfaces have peaks at approximately 490 and 590 nm (corresponding to blue and yellow), which may originate from the characteristics of the material or pigments used in the 3D printing (see also Sect. 3.2). The mean RMSE and SSV over the 110 colour patches was 0.00349 (SD 0.0026) and 0.431 (SD 0.076), respectively. These values can serve as a baseline for evaluating the spectra in 2D and 3D printings in the following sections. Although the colour profiling in the manufacturing process was based only on the CIE tristimulus values, the errors in the spectral reproduction were as small as the reported errors in the colour reproduction [21].

5 Analysis of facial prostheses

5.1 Colorimetric analysis

The chromaticity coordinates a^*b^* of the subjects with Caucasian skin or Chinese skin (both forehead and cheek) were computed from spectral reflectances. The chromaticity coordinates of the ground-truth skin and manufactured skin prostheses of the three subjects are shown in Fig. 2c, d, with the colour gamut shown in Fig. 2a, b. Triangles and circles represent forehead and cheek samples, respectively. Filled and open symbols represent 2D and 3D printed faces, respectively, whereas the filled grey symbols represent the ground truth. The reproductions had larger differences compared to the ground truth on the forehead for all the three subjects, regardless of the skin type (Caucasian or Chinese). Additionally, the distribution of the chromaticity coordinates over the colour gamut was dependent on the skin types and the areas measured.

5.2 Facial prostheses in 3D and 2D

Figure 4 shows one of the Chinese subjects with the 2D and 3D manufactured faces. (One of the co-authors was one of the two Chinese subjects; pictures shown with permission.) This demonstrates that the colour appearances of the 2D and 3D surfaces are different even though the same printing method was used.

The colour difference CIEDE2000 between each skin prosthesis and the corresponding ground-truth skin under the standard illuminant D65 was computed on each of the forehead and cheek areas (Fig. 5). There were variations between the skin types, subjects and measured areas. These differences were not consistent over the subjects and skin areas, although

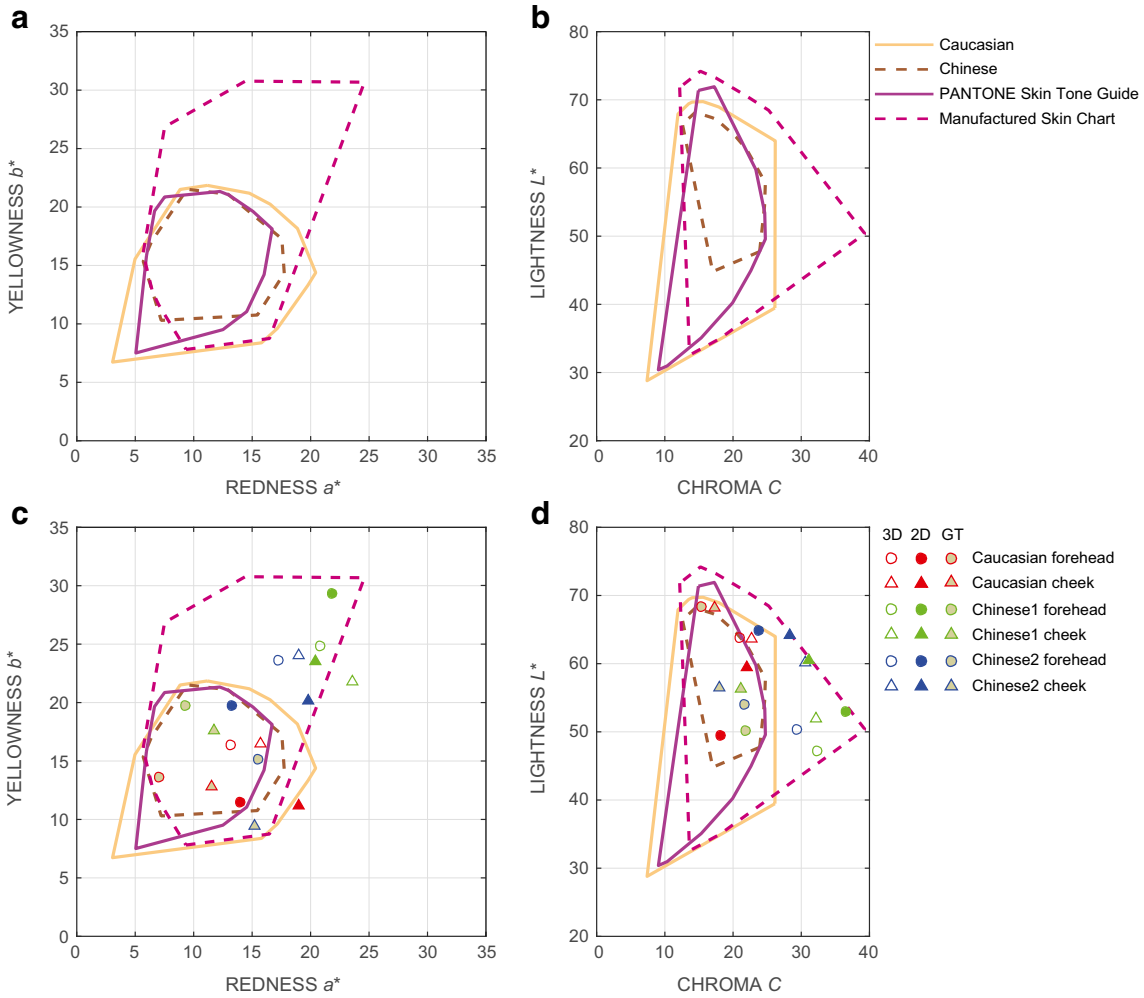

Fig. 2 Colour gamut and printed skin samples. **a** Yellowness vs Redness for real skin (caucasian and chinese), for the PANTONE skin guide and for the printed skin chart. **b** Lightness vs Chroma for real skin (caucasian and chinese), for the PANTONE skin guide and for the printed skin chart. **c** same as (a) but also with colorimetric values of printed skin (3D and 2D) and ground truth (GT) values of real human skin. **d** same as (b) but with colorimetric values of printed skin (3D and 2D) and ground truth (GT) values of real human skin included

the reproduction in 3D tended to have smaller errors relative to the ground-truth skin when compared to 2D.

The values of the CIEDE2000 in the forehead area were 6.5 for the Caucasian subject and 7.15 for the average of the two Chinese subjects (each 8.2 and 6.1). The values were larger with the 2D prostheses. The Caucasian subject had the largest error of 18.5, whereas the Chinese subjects had errors of 8.5 and 10.4, respectively. For the cheek area, the CIEDE2000

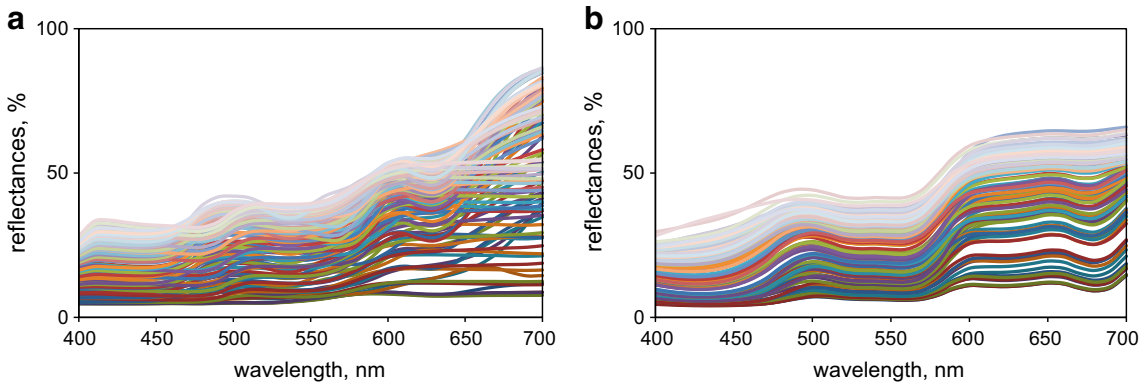

Fig. 3 Differences in spectral profiles **a** The reflectance spectra of the PANTONE Skin Tone Guide. **b** The reflectance spectra of the additively manufactured skin colour chart

Fig. 4 Prostheses from left to right, the camera image, the 3D printed and the 2D printed face of one of the chinese observers is shown

values were 5.1 and 8.9 (the average of the values for two subjects, 8.4 and 9.4) in 3D for the Caucasian subject and Chinese subjects, respectively. In 2D, the values were 9.9 for Caucasian skin and 8.1 for the average Chinese skin (6.8 and 9.3). Thus, there were large differences between the 3D- and 2D-printed surfaces, particularly on the Caucasian subject's forehead. The potential causes of the errors between the 3D and 2D manufacturing results are considered in the discussion.

5.3 Colours under different illuminants

When considering the practical situation of applying facial prostheses to patients, the colour difference between the patient's skin and the prosthesis should not be influenced by scene illuminations. However, the colour appearance of facial prostheses does vary with different illumination, and this effect must be considered for the practical application of the prostheses.

Colorimetric analysis was repeated with the simulation of different illuminations on the skin surfaces. A range of the CIE standard illuminants were simulated: CIE standard daylight A, D50, D65 and florescent lights (F1, F3, F7, F10 and F11). The colour difference CIEDE2000 was calculated against the ground truth of each subject's skin under the standard illuminant D65.

Figure 6 demonstrates the CIEDE2000 of the 3D prostheses with the Caucasian and Chinese skin types. The forehead and cheek areas and their averages are shown in the different columns. The CIEDE2000 ranged over 3.5–6.9 for the Caucasian skin type and 4.5–9.2 for the Chinese skin type. The errors on the Chinese skin type were slightly higher than those for the Caucasian skin type. The CIEDE2000 values varied depending on the illumination, but overall the average was 3.4 for Caucasian and 4.8 for Chinese, which are close to the acceptable value.

The consistent colour appearance of surfaces under different illuminations is one of the critical factors to be considered in the application of facial prostheses to patients. The perceptual colour difference between the prosthetic and surrounding real skin should be minimal and consistent during changes in scene illumination. For this practical consideration, the achievement of colour constancy would indicate the quality of colour management in the manufacturing process of the prosthesis.

Colour-constancy performance has been assessed by the reproduction colour-constancy index, which is defined in a

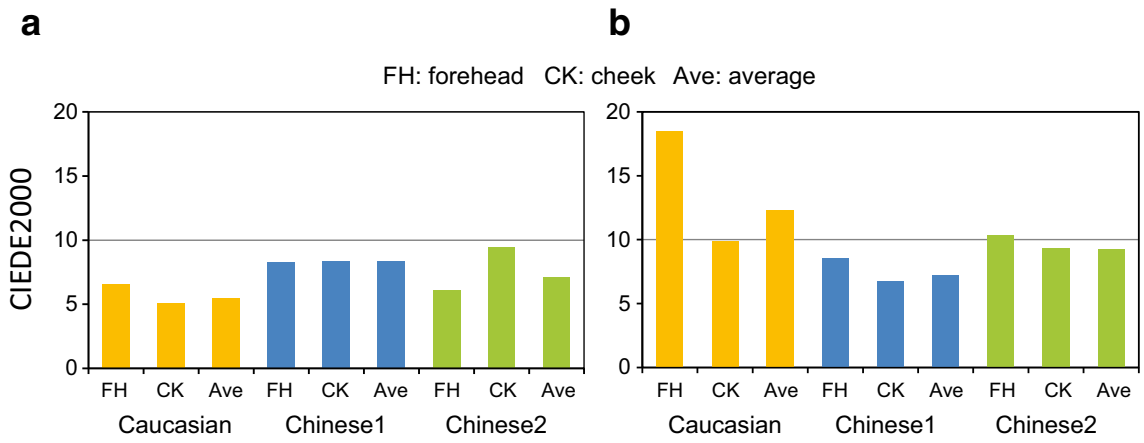

Fig. 5 CIE DE2000: vs. ground truth **a** The perceptual colour difference between the 3D printed skin and the ground truth (original face) is shown for the forehead (FH) and the cheek (CK) for the three participants (Caucasian, Chinese1 and Chinese2). **b** as in (a) but for 2D printed faces.

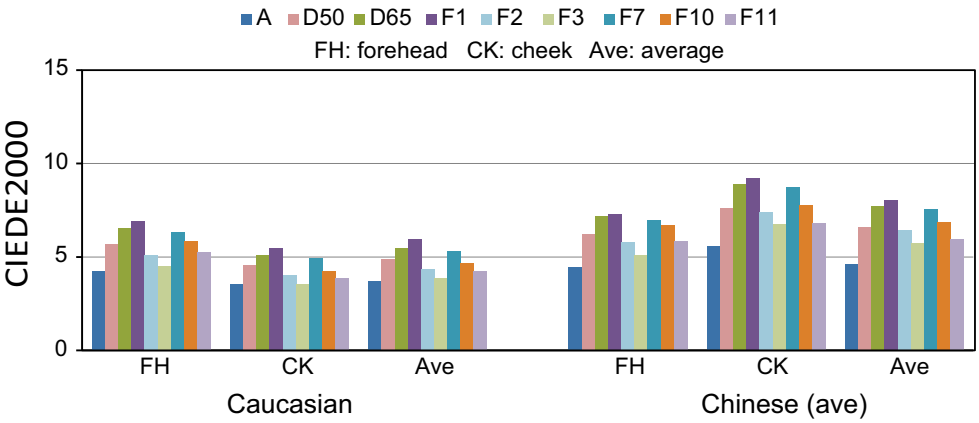

Fig. 6 CIEDE2000 under different illuminations. Perceptual colour differences are plotted for the forehead (FH) and the cheek (CK) for the caucasian (left set of bars) and the average chinese participant (right set of bars). Different coloured bars denote the perceptual error when the skin is rendered under different illuminations (A, D50, D65, F1, F2, F3, F7, F10, F11)

similar manner as the standard colour-constancy index established in vision sciences [39, 45]. Thus, in the colour space where the chromaticity coordinates of real skin and manufactured skin were located (here, the CIE $L^*a^*b^*$), let a be the distance between the colour of the real skin and colour of the prosthetic under a test illuminant and b be the distance between the real skin colours under the reference and test illuminations. Then, the reproduction colour-constancy index is $1 - a/b$. Perfect constancy corresponds to unity, and the index is lower for a higher error level (Fig. 7).

In this study, the distances are replaced with the CIEDE2000, and two directions of the illumination changes between the reference and test were considered. Figure 8 shows the shifts of the chromaticity distributions of the real faces and prostheses under the D65, A and F2 illuminants. As shown in Fig. 7, the colour of the prosthesis under the reference illuminant is not considered in the calculation of the index in a direction of illumination changes, which may generate bias in the evaluation of colour-constancy performance. To prevent such bias, both directions of the illumination changes were considered by reversing the reference illuminant and test illuminant.

The results are summarised in Fig. 9. The pairs of illuminations considered were the CIE standard illuminants A and D65 and F2 and D65. Both directions of the illumination changes, namely from and to D65, can be considered. The values of the averaged reproduction colour-constancy index ranged from 0.46 to 0.76. The indices for the 2D prostheses tended to be lower than those for the 3D prostheses. The worst performance was on the Caucasian subject's 2D forehead, which may be explained by the larger errors in colour difference (Fig. 5). The values obtained here are close to the values obtained in colour-constancy experiments by human observers [45]. Despite the colour differences among skin areas of individuals, these achievements are useful for the practical application of skin prostheses.

5.4 Individual differences (difference from the means)

As shown in Fig. 2c, the three subjects had different chromaticity coordinates from the mean chromaticity. The colour difference CIEDE2000 under D65 on the cheek was 6.1 for the Caucasian subject and 3.5 and 7.4 for the two Chinese subjects. These deviations from the mean colours and the offset between the Skin Tone Guide and Skin Chart (Sect. 2.1)

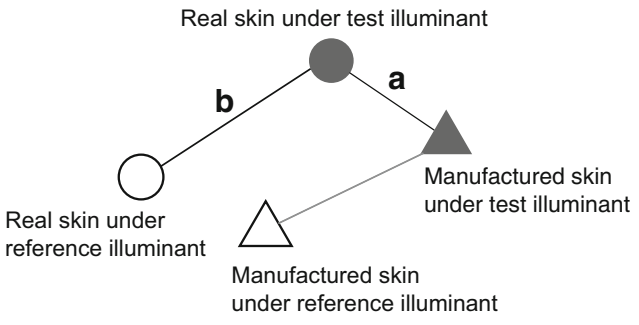

Fig. 7 Schematic diagram of the definition of the reproduction colour-constancy index (RCCI). The RCCI captures the colour quality of the printed skin in relation to the invariance of real skin under different illumination conditions

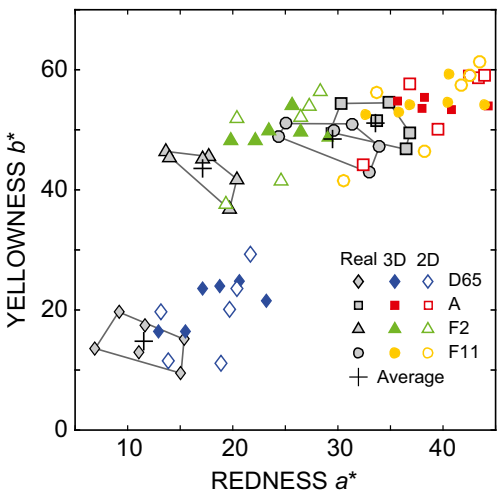

Fig. 8 Shift in the chromaticity distributions

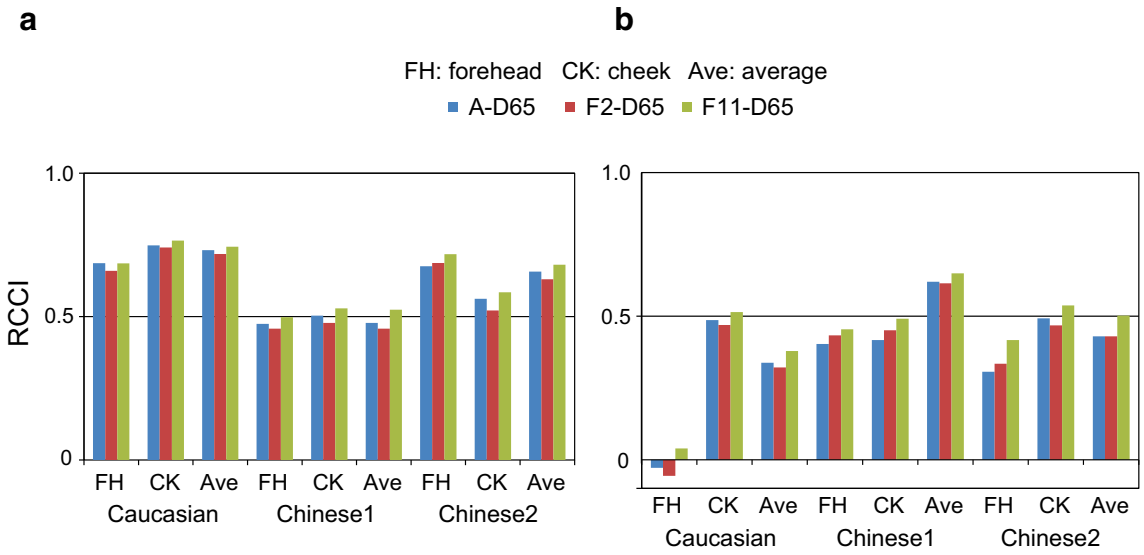

Fig. 9 Reproduction colour-constancy index **a** The RCCI is shown for the 3D printed skin for both ethnicities for the forehead (FH) and and the cheek (CK). Coloured bars denote the RCCI under different illumination changes: from illuminant A to D65 (blue); from F2 to D65 (red); from F11 to D65 (green). **b** same as (a) but for the 2D printed skin

must be considered to interpret the CIEDE2000 values, rather than considering only the general acceptable difference, namely, 3–4. That is, the range of CIEDE2000 under different illuminations should be close to the acceptable range.

6 Spectral analysis of facial prostheses

6.1 Spectral characteristics of individual faces

Spectral reflectances of the human subjects' real skin and 3D- and 2D-printed skins were evaluated. There are variations in spectral profiles between the three individuals, between skin types (Caucasian and Chinese) and between face regions. Interestingly, the characteristics are comparable to those identified in the earlier report with larger samples [43]. However, as noted in Sect. 5.4, the variations in skin colour of the three subjects in the present study from the mean colour of each skin type were evident. There were large variations in spectral properties between printed 3D and 2D skins, subjects and areas of the face.

As with the Skin Chart, the spectral characteristics of the manufactured faces have peaks around 490 and 590 nm (Fig. 3). The variation of each spectra relative to the ground truth was evaluated by the RMSE and SSV, as in Sect. 4.2.1. The RMSE and SSV were computed with each individual's ground-truth skin reflectances (Tables 2 and 3).

The RMSE and SSV between the printed faces and ground truth for the three individual subjects are summarised in Table 2. The results demonstrated that similar RMSE and

Table 3 RMSE and SSV (spectral similarity value) on 3D and 2D prostheses to ground truth

		3D		2D	
Subject		RMSE	SSV	RMSE	SSV
Caucasian	Forehead	0.0580	0.3096	0.2012	0.4040
	Cheek	0.0632	0.2953	0.1016	0.3296
	Average	0.0612	0.2977	0.1344	0.3499
Chinese1	Forehead	0.0350	0.3429	0.0751	0.3474
	Cheek	0.0427	0.3233	0.0784	0.3219
	Average	0.0393	0.3274	0.0767	0.3268
Chinese2	Forehead	0.0542	0.3270	0.1057	0.3589
	Cheek	0.0595	0.3668	0.0983	0.3694
	Average	0.0386	0.3405	0.1029	0.3560
Mean		0.0502	0.3256	0.1083	0.3515
Std.dev.		0.0111	0.0229	0.0395	0.0253

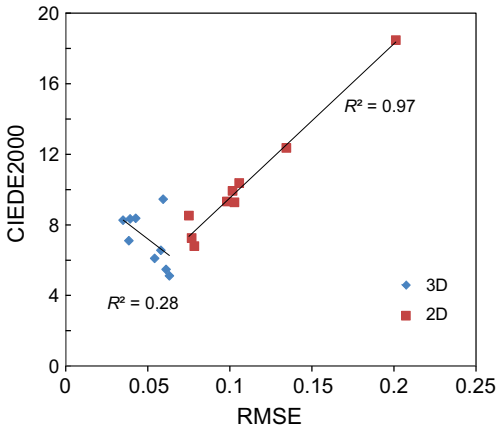

Fig. 10 RMSE vs. CIEDE2000

SSV levels were achieved when compared to the study investigating spectral reconstruction of human skin from RGB digital values [42].

6.2 Correlation between the RMSE and colour difference

Are the colour differences related to spectral differences? CIEDE2000 colour differences between the real and manufactured skin surfaces under D65 illuminant were plotted as a function of the RMSE of the spectral characteristics. The relationships between them were quantified by the correlation coefficient of determination R^2.

The correlation coefficients were 0.28 and 0.97 for the 3D and 2D surfaces, respectively (Fig. 10). Although the 2D surfaces have a higher correlation coefficient, the colour difference and the perceptual differences between the manufactured and real skin were larger than for 3D surfaces. The values on the intercept of the regression line on the CIEDE2000 axis could be considered the bias in manufacturing. Ideally, if the spectral error (RMSE) is zero, the colour difference (CIEDE2000) between the ground truth and prosthesis should be zero. The intercepts of the 3D and 2D prostheses are 10.8 and 0.8, respectively. For the 2D surfaces, the evaluation of the CIEDE2000 relative to the ground-truth skin in Sect. 4.2 could be considered (here, the 3D surfaces could not be considered because there were no correlations). When the intercept was forced to be zero, the linear regression failed with the 3D prostheses but achieved a higher R^2 of 0.97 with the 2D prostheses.

7 Discussion

The quality of colour reproduction in the 3D facial prostheses produced by additive manufacturing was assessed using a perceptual error formula, namely, CIEDE2000, and spectral analysis, using RMSE and SSV. The prostheses were based on a Caucasian female and two Chinese male individuals using the specially designed colour management profile. In addition, colour reproduction under different illuminations was evaluated. Considering the offset in the colour management and individual differences, the colour difference with the 3D prostheses ranged over 5–9, which is demonstrably larger than the acceptable error range of 3–4 in CIEDE2000. Colour constancy of the prosthesis surfaces was assessed with the standard colour-constancy index [39, 45]. The level of the reproduction constancy index, measured with the constancy index, was similar to the results obtained by human observers in colour matching experiments [45]. However, there were variations in performance between the individual subjects, skin types (one Caucasian and two Chinese) and areas of the measurements. Furthermore, the maximum achievable constancy was limited by the choice of illumination [40].

Compared to ground-truth data, namely, real human skin, the colour reproduction of the facial prostheses was not perfect and fell short of the optimal outcome required. Errors were observed in both the colorimetric and spectral assessments. Potential causes of the errors might lie within the colour management process or limits in hardware performance. Additionally, consistency in the measurement of the human skin is often difficult to achieve due to the variations in physiological condition (body temperature, sweat, emotional arousal, nonflat surfaces, hydration and movement [6, 46]) and physical condition (surface curvatures, nonuniformity, surface texture and diseases). Therefore, measurements may only be representative of that point in time or environment, particularly under extreme external conditions. However, investigating these variations even under relatively "standard" conditions posed some difficulty.

Acknowledgements Some of the results were reported at the 17th Vision Sciences Society Annual Meeting, 19–24 May 2017, St. Pete Beach, FL., USA.

Funding information This work was supported by the Engineering and Physical Sciences Research Council, UK (Grants EP/L001012/1 and EP/K040057).

Compliance with ethical standards All experiments were conducted following approval by the University of Liverpool Research Ethics Committee, which operates in accordance with the Declaration of Helsinki. Signed consent was obtained from each subject who took part in the measurements.

Conflict of interest The authors declare that they have no conflict of interest.

References

1. De Rigal J, Des Mazis I, Diridollou S, Querleux B, Yang G, Leroy F, Barbosa VH (2010) The effect of age on skin color and color heterogeneity in four ethnic groups. Skin Res Technol 16(2):168–178. https://doi.org/10.1111/j.1600-0846.2009.00416.x
2. Ramirez GA, Fuentes O, Crites SL, Jimenez M, Ordonez J (2014) Color analysis of facial skin: detection of emotional state. In: 2014 I.E. Conference on Computer Vision and Pattern Recognition Workshops, 23–28 June 2014. pp 474–479. doi: https://doi.org/10.1109/CVPRW.2014.76
3. Chen T, Yuen P, Richardson M, Liu G, She Z (2014) Detection of psychological stress using a hyperspectral imaging technique. IEEE Trans Affect Comput 5(4):391–405. https://doi.org/10.1109/TAFFC.2014.2362513
4. Da Pos, Green-Armytage P (2007) Facial expressions, colours and basic emotions. J Int Colour Assoc 1(2):1–20

5. Frith C (2009) Role of facial expressions in social interactions. Philos Trans R Soc Lond Ser B Biol Sci 364(1535):3453–3458. https://doi.org/10.1098/rstb.2009.0142
6. Changizi MA, Zhang Q, Shimojo S (2006) Bare skin, blood and the evolution of primate colour vision. Biol Lett 2(2):217–221. https://doi.org/10.1098/rsbl.2006.0440
7. Jimenez J, Scully T, Barbosa N, Donner C, Alvarez X, Vieira T, Matts P, Orvalho V, Gutierrez D, Weyrich T (2010) A practical appearance model for dynamic facial color. ACM Trans Graph 29(6):141. https://doi.org/10.1145/1882261.1866167
8. Paravina RD, Majkic G, Del Mar PM, Kiat-amnuay S (2009) Color difference thresholds of maxillofacial skin replications. J Prosthodont 18(7):618–625. https://doi.org/10.1111/j.1532-849X.2009.00465.x
9. Xiao K, Zardawi F, van Noort R, Yates JM (2014) Developing a 3D colour image reproduction system for additive manufacturing of facial prostheses. Int J Adv Manuf Technol 70(9–12):2043–2049. https://doi.org/10.1007/s00170-013-5448-1
10. Xiao K, Wuerger S, Mostafa F, Sohaib A, Yates JM (2016) Colour image reproduction for 3D printing facial prostheses. New trends in 3D printing. InTech. https://doi.org/10.5772/63339
11. MacGreggor FC (1951) Some psycho-social problems associated with facial deformities. Am Sociol Rev 16(5):629–638. https://doi.org/10.2307/2087355
12. Bailey LW, Edwards D (1975) Psychological considerations in maxillofacial prosthetics. J Prosthet Dent 34(5):533–538. https://doi.org/10.1016/0022-3913(75)90041-4
13. Gillis RE Jr, Swenson WM, Laney WR (1979) Psychological factors involved in maxillofacial prosthetics. J Prosthet Dent 41(2):183–188. https://doi.org/10.1016/0022-3913(79)90305-6
14. Sachs E, Vezzetti E (2005) Numerical simulation of deposition process for a new 3DP printhead design. J Mater Process Technol 161(3):509–515. https://doi.org/10.1016/j.jmatprotec.2004.07.090
15. Curodeau A, Sachs E, Caldarise S (2000) Design and fabrication of cast orthopedic implants with freeform surface textures from 3-D printed ceramic shell. J Biomed Mater Res 53(5):525–535. https://doi.org/10.1002/1097-4636(200009)53:5<525::AID-JBM12>3.0.CO;2-1
16. Zardawi FM, Xiao K, van Noort R, Yates JM (2015) Investigation of elastomer infiltration into 3D printed facial soft tissue prostheses. Anaplastology 4(1):2161–1173. https://doi.org/10.4172/2161-1173.1000139
17. Hungerford E, Beatty MW, Marx DB, Simetich B, Wee AG (2013) Coverage error of commercial skin pigments as compared to human facial skin tones. J Dent 41(11):986–991. https://doi.org/10.1016/j.jdent.2013.07.010
18. Xiao K, Zardawi F, van Noort R, Yates JM (2013) Color reproduction for advanced manufacture of soft tissue prostheses. J Dent 41(Suppl 5):e15–e23. https://doi.org/10.1016/j.jdent.2013.04.008
19. Zardawi FM, Xiao K, van Noort R, Yates JM (2015) Mechanical properties of 3D printed facial prostheses compared to handmade silicone polymer prostheses. Eur Sci J 11(12):1–11
20. Pantone LLC (2012) PANTONE SkinTone™ Guide. Carlstadt, NJ, USA
21. Xiao K, Yates JM, Zardawi F, Sueeprasan S, Liao N, Gill L, Li C, Wuerger S (2017) Characterising the variations in ethnic skin colours: a new calibrated data base for human skin. Skin Res Technol 23(1):21–29. https://doi.org/10.1111/srt.12295
22. Gozalo-Diaz DJ, Lindsey DT, Johnston WM, Wee AG (2007) Measurement of color for craniofacial structures using a 45/0-degree optical configuration. J Prosthet Dent 97(1):45–53. https://doi.org/10.1016/j.prosdent.2006.10.013
23. Zonios G, Bykowski J, Kollias N (2001) Skin melanin, hemoglobin, and light scattering properties can be quantitatively assessed in vivo using diffuse reflectance spectroscopy. J Invest Dermatol 117(6):1452–1457. https://doi.org/10.1046/j.0022-202x.2001.01577.x
24. Anderson RR, Parrish JA (1981) The optics of human skin. J Invest Dermatol 77(1):13–19. https://doi.org/10.1111/1523-1747.ep12479191
25. Park J-H, Lee Y-K, Lim B-S (2006) Influence of illuminants on the color distribution of shade guides. J Prosthet Dent 96(6):402–411. https://doi.org/10.1016/j.prosdent.2006.10.007
26. CIE, Technical Committee 1–48 (2004) Colorimetry, 3rd edn. Commission Internationale de l'Eclairage, Vienna, Austria
27. Sharma G, Wu W, Dalal EN (2005) The CIEDE2000 color-difference formula: implementation notes, supplementary test data, and mathematical observations. Color Res Appl 30(1):21–30. https://doi.org/10.1002/col.20070
28. Sweet J, Granahan J, M. Sharp (2000) An objective standard for hyperspectral image quality. In: Proceedings of AVIRIS workshop, jet propulsion laboratory, Pasadena, California. Jet Propulsion Laboratory, California Institute of Technology
29. Shrestha R, Pillay R, George S, Hardeberg JY (2014) Quality evaluation in spectral imaging—quality factors and metrics. J Int Colour Assoc 12:22–35
30. Gozalo-Diaz D, Johnston WM, Wee AG (2008) Estimating the color of maxillary central incisors based on age and gender. J Prosthet Dent 100(2):93–98. https://doi.org/10.1016/S0022-3913(08)60155-9
31. Koran A, Powers JM, Raptis CN, Yu R (1981) Reflection spectrophotometry of facial skin. J Dent Res 60(6):979–982. https://doi.org/10.1177/00220345810600061301
32. Caisey L, Grangeat F, Lemasson A, Talabot J, Voirin A (2006) Skin color and makeup strategies of women from different ethnic groups. Int J Cosmet Sci 28(6):427–437. https://doi.org/10.1111/j.1467-2494.2006.00329.x
33. Hong G, Luo MR, Rhodes PA (2001) A study of digital camera colorimetric characterization based on polynomial modeling. Color Res Appl 26(1):76–84. https://doi.org/10.1002/1520-6378(200102)26:1<76::AID-COL8>3.0.CO;2-3
34. Chauhan T, Xiao K, Yates J, Wuerger S (2015) Estimating discrimination ellipsoids for skin images. J Vis 15(12):820. https://doi.org/10.1167/15.12.820
35. Ahn J-S, Lee Y-K (2008) Color distribution of a shade guide in the value, chroma, and hue scale. J Prosthet Dent 100(1):18–28. https://doi.org/10.1016/S0022-3913(08)60129-8
36. Lee Y-K, Yu B, Lim H-N (2010) Lightness, chroma, and hue distributions of a shade guide as measured by a spectroradiometer. J Prosthet Dent 104(3):173–181. https://doi.org/10.1016/S0022-3913(10)60116-3
37. Melgosa M, Alman DH, Grosman M, Gómez-Robledo L, Trémeau A, Cui G, García PA, Vázquez D, Li C, Luo MR (2013) Practical demonstration of the CIEDE2000 corrections to CIELAB using a small set of sample pairs. Color Res Appl 38(6):429–436. https://doi.org/10.1002/col.21751
38. CIE (2008) CIE Standard llluminants for Colorimetry. S 014-2/E:2006/ISO 11664-2:2007(E). Commission Internationale de L'Eclairage, Vienna, Austria
39. Arend LE, Reeves A, Schirillo J, Goldstein R (1991) Simultaneous color constancy: papers with diverse Munsell values. J Opt Soc Am A 8(4):661–672. https://doi.org/10.1364/JOSAA.8.000661
40. Amano K, Sohaib A, Xiao K, Yates JM, Whitford C, Wuerger SM (2017) Color quality assessments of 3D facial prostheses in varying illuminations. Paper presented at the Vision Sciences Society Annual Meeting, St Pete Beach, 19-24 May 2017
41. Wang M, Xiao K, Luo R, Zhu Y, Wuerger S Investigation of uncertainty of skin colour measurements. In: Proceedings of the 28th Session of the CIE, 28 June - 4 July 2015, Manchester, UK, 07/01/2015
42. Xiao K, Zhu Y, Li C, Connah D, Yates JM, Wuerger S (2016) Improved method for skin reflectance reconstruction from camera

images. Opt Express 24(13):14934–14950. https://doi.org/10.1364/OE.24.014934
43. Xiao K, Wang M, Luo R, Li C, Wuerger S (2016) Characterisation of skin spectra in a Caucasian and Oriental sample. Electron Imaging 2016(20):1–4. https://doi.org/10.2352/ISSN.2470-1173.2016.20.COLOR-338
44. Sinthanayothin C, Bholsithi W (2005) Image warping based on 3D thin plate spline. Paper presented at the International Conference on Information Technology in Asia 2005, Sarawak, Malaysia., December 12-15, 2005
45. Foster DH (2011) Color constancy. Vis Res 51(7):674–700. https://doi.org/10.1016/j.visres.2010.09.006
46. Alkawaz MH, Mohamad D, Saba T, Basori AH, Rehman A (2015) The correlation between blood oxygenation effects and human emotion towards facial skin colour of virtual human. 3D. Research 6(2):13. https://doi.org/10.1007/s13319-015-0044-9